A Wave Function Correction-Based Approach to the Identification of Resonances for Vibrational Perturbation Theory

Mark A. Boyer[1] and Anne B. McCoy[1, a)]

Department of Chemistry, University of Washington, Seattle, WA 98195, USA

(Dated: 16 September 2022)

An approach for identifying resonances in vibrational perturbation theory calculations is introduced. This approach makes use of the corrections to the wave functions that are obtained from non-degenerate perturbation theory calculations to identify spaces of states that must be treated with degenerate perturbation theory. Pairs of states are considered to be in resonance if the magnitude of expansion coefficients in the corrections to the wave functions in the non-degenerate perturbation theory calculation are greater than a specified threshold, $\chi^{\max}$. This approach is applied to calculations of the vibrational spectra of CH_4, H_2CO, HNO_3, and cc-HOONO. The question of how the identified resonances depend on the value of $\chi^{\max}$ and how the choice of the resonance spaces affects the calculated vibrational spectrum is further explored for H_2CO. The approach is also compared to the Martin test [J. Chem. Phys. **103**, 2589-2602 (1995)] for calculations of the vibrational spectra of H_2CO and cc-HOONO.

a)Electronic mail: abmccoy@uw.edu

I. INTRODUCTION

The simulation of vibrational spectra is a key element in the process of making connections between experimentally observable quantities and the fundamental physics of molecular systems.[1–3] There are many highly-accurate approaches that have been taken to simulate such spectra. Methods like discrete variable representations[4,5] (DVR) and local-mode models[6–8] (LMM) are used to provide accurate descriptions of individual coordinates. These representations of single oscillators may then be combined via direct-product bases or similar approaches to obtain a representation of the full-dimensional Hamiltonian.[4,5,9–11] Unfortunately, due to the so-called "curse of dimensionality," these simple approaches works best only for small systems or in reduced-dimensional models. In extending these types of techniques to higher-dimensional problems, it is common to use approaches like the vibrational self-consistent field/vibrational configuration interaction (VSCF/VCI) method[12–14] and the multiconfiguration time-dependent Hartree (MCTDH) method,[14–16] which make use of DVRs and LMMs to obtain full-dimensional solutions to the Schrödinger equation. These methods provide high-quality spectral information, but can come at a considerable computational cost. Moreover, these methods require a full potential energy surface that spans the entirety of the relevant configuration space for the system of interest.

As a complement to these highly-accurate but expensive methods, more approximate methods also exist, the best-known likely being the harmonic oscillator model. In the harmonic approximation, the potential energy is approximated by a second-order Taylor series about the minimum-energy geometry. The vibrational Hamiltonian for an N-atom system can then be expressed as

$$H = \sum_{i=1}^{3N-6} \frac{\omega_i}{2}(p_i^2 + q_i^2), \tag{1}$$

where the q_i are the $3N-6$ normal modes and the p_i are the momenta conjugate to the normal modes.

For systems where a quadratic approximation to the potential works well—a common case for systems with small-amplitude motions—the harmonic approximation, potentially with scaling factors,[17] provides a good zero-order solution to the full vibrational Schrödinger equation. However, for systems with significant anharmonicity, a better solution is obtained through vibrational perturbation theory (VPT).[18–25] The power of vibrational perturbation theory is illustrated by the Morse potential,[26] for which the energy levels can be expressed as

a quadratic expansion in $(n + 1/2)$. When this model potential is expanded through fourth order in the bond displacement and second-order vibrational perturbation theory (VPT2) is used to evaluate the energies, the VPT2 calculation will provide the exact values for these energies. On the other hand, a variational calculation that uses this quartic expansion of the potential will show notable deviations from the expected energies. Comparing the corrections to the energies from VPT2 to energies obtained from a variational calculation that is based on a quartic expansion of a Morse potential that describes an OH oscillator, with $\omega = 3869.47$ cm^{-1} and $\omega x = -84.11$ cm^{-1},[23] one finds that the variational calculation overestimates the energies of the states with one and two quanta of excitation by 30 and 150 cm^{-1}, respectively (an error of 1% and 4%). As the potential energy for stretching vibrations is often well-approximated by a Morse potential, a VPT2 calculation that is based on a quartic expansion of the potential is anticipated to provide more accurate energies for the stretching vibrations than a variational calculation that utilizes the same truncated expansion of the potential.

On the other hand, in the presence of resonance interactions,[1,18,27] VPT is known to display large errors in the corrections to the energies and other properties. In the context of vibrational perturbation theory, resonances occur when the expansions of the energies and wave functions used in the perturbation theory do not converge. Formally, resonances can occur when the couplings between states become too large, but most commonly they occur when the zero-order states are degenerate or nearly-degenerate. At second order, the most problematic such resonances will be those that involve cubic terms in the expansion of the Hamiltonian, a common example of which is the 2:1 Fermi resonance between states with two quanta in a bending vibration and one in a stretching vibration. Such resonances are handled via the deperturb-and-diagonalize method, where terms that couple resonant states are discarded when performing the perturbation theory calculation and reintroduced in the subsequent variational step.[18,25,27–32] Following the previous discussions of this approach,[24,31,33] we will refer to the approach where no resonances are handled—i.e. where no terms are discarded—as non-degenerate or standard perturbation theory (SVPT), the approach where the terms that couple resonant states are discarded as deperturbed vibrational perturbation theory (DVPT), and the case where these terms are then reintroduced via a variational step, i.e. the deperturbed-and-diagonalized approach, as generalized vibrational perturbation theory (GVPT). GVPT, while effective, requires resonances to be

identified so that the effects of the resonances may be properly accounted for.

It is sometimes possible to identify resonances *a priori*. For example, what is now known as Fermi resonance was first discussed by Fermi and subsequently applied to a study of CO_2 by Fermi and Dennison.[34] In that work, it was noted that the frequency of the fundamental in the symmetric CO stretching vibration was almost exactly twice the frequency of the doubly-degenerate OCO bending modes. In later studies, collective quantum numbers have also been used to account for more complicated polyads of resonances.[30,35–37] Recasting the prior discussion in terms of a collective quantum number, for CO_2 one can define

$$N_t = 2n_{\mathrm{CO}} + n_{\mathrm{OCO}}, \tag{2}$$

where n_{CO} is the number of quanta of excitation in the symmetric CO stretch and n_{OCO} provides the number of quanta in the doubly-degenerate OCO bend. All states with the same value of N_t will be considered to be in resonance. For example, the state with one quantum of excitation in the symmetric CO stretch is in resonance with the states with two quanta of excitation in the OCO bends.

In the absence of prior knowledge of the important resonances in a system, more automated approaches are required. One approach, used by Handy and coworkers in the development of the SPECTRO program,[38] is to determine that a pair of states is in resonance if the difference between zero-order energies of these states is less than a supplied threshold. Another approach, which is used in the implementation of vibrational perturbation theory in the CFOUR[39] package, uses the derivatives of the VPT2 energies with respect to the harmonic frequencies of the states to determine if a pair of states is in resonance.[40] Krasnoshchekov and coworkers have investigated criteria for the identification of resonances based on the size of terms in the expansion of the transformation operator used in canonical Van Vleck perturbation theory.[41] However, the most widely-used approach for identifying important resonance interactions is the Martin Test.[42] The working equation for the Martin test is obtained by considering the two-by-two coupling matrix involving states $|n\rangle$ and $|m\rangle$, with the energy of the deperturbed states, E_n^* and E_m^*, on the diagonal and the coupling between these two states, which is obtained from cubic terms in the Hamiltonian, on the off-diagonal. The energies obtained by applying perturbation theory to this matrix are then compared to those obtained from a Taylor series expansion of the eigenvalues of the matrix. If the leading term in the differences between these two sets of calculated energies exceeds a

specified threshold, χ^{Martin}, the states are determined to be in resonance. A common choice for χ^{Martin} is 1 cm^{-1}, although values as large as 10 cm^{-1} and as small as 0.1 cm^{-1} have been reported.[24,25]

The Martin test provides a reliable diagnostic. It is the approach that is implemented in the Gaussian 16 software package, and has been recently discussed by Barone and coworkers in the context of a recent study of astrochemical molecules.[43,44] However, it is limited to pairs of states that are coupled by cubic terms in the expansion of the Hamiltonian. Resonances involving states with the same total number of quanta of excitation, also known as Darling-Dennison resonances,[45] must be identified by other approaches. This is commonly done by comparing the difference between the energies of the proposed nearly degenerate states to a threshold value,[43] as described above and implemented in SPECTRO.

Automated approaches are, in general, very successful at accounting for resonances that lead to divergent expansions in the perturbation theory calculation. It is worth noting, however, that many resonances have more subtle effects and the identification of such resonances can lead to important changes in the calculated spectrum. For example, in a recent study of isoprene,[25] Stanton and coworkers found that the simulated spectrum that was obtained from GVPT2 calculations was sensitive to the choice of resonances. In that study, the best agreement with the experimental spectrum was obtained by including not only those resonances identified by the Martin test (for Fermi resonances) and an energy window (for Darling-Dennison resonances), but by also including resonances between all of the CH scissoring modes. This mixture of an automated approach with *a priori* information provided a high-fidelity reproduction of the experimental spectrum for isoprene.

Most automated approaches to resonance identification (energy windows, harmonic derivatives, and the Martin test) discussed above, are all focused on the VPT corrections to the energies. This focus on energies is not ideal, as Stanton and coworkers have noted that VPT corrections to the transition moments can be more sensitive to resonances than the corrections to the energies.[46]

On the other hand, the focus on the energies in the identification of resonances is entirely logical. For efficiency reasons, most implementations of vibrational perturbation theory build off of work by Nielsen and coworkers and use analytic expressions for the corrections to the energies and transition moments, with the deperturbed corrections to the energies and transition moments obtained by modifying these expressions.[24,46–49] This means that

corrections to the wave functions are rarely evaluated. By contrast, in a recent paper[50] (hereafter referred to as Paper I) we described an implementation of VPT that builds off of work by Kato[51] and Sakurai.[33] This approach utilizes sparse linear algebra approaches to solve the equations in perturbation theory numerically. This allows us to keep track of corrections to the wave functions as well as the energies. We have used the approach to perform GVPT calculations as part of studies of the $CH_2(CH_3)_2COOH$ radical,[52] complexes of halide ions with HOCl,[53] and the Cl^-·HOI complex.[54] In performing these studies, we utilized prior knowledge and chemical intuition to determine which resonances needed to be accounted for in the GVPT calculations. In the present study, we explore an automated approach to the identification of resonances that exploits the ability to obtain corrections to the wave functions. This approach for identifying resonances provides the beneficial features of the Martin test and energy window approaches while also allowing for the identification of more subtle resonances that manifest more strongly in the corrections to the intensities than the energies.

II. THEORY

In vibrational perturbation theory, the Hamiltonian is expanded as a Taylor series in the normal mode coordinates as

$$H = \lambda^0 H^{(0)} + \lambda^1 H^{(1)} + \lambda^2 H^{(2)} + \cdots \ . \tag{3}$$

Here $H^{(0)}$ is the separable harmonic Hamiltonian, including the terms that are quadratic in the normal mode coordinates, q, and the conjugate momenta, p. The cubic terms in p and q are included in $H^{(1)}$, the quartic terms are in $H^{(2)}$, and so forth. The wave functions and energies are also expanded as a formal power series in λ as

$$|n\rangle = \lambda^0 |n^{(0)}\rangle + \lambda^1 |n^{(1)}\rangle + \lambda^2 |n^{(2)}\rangle + \cdots \tag{4}$$

$$E_n = \lambda^0 E_n^{(0)} + \lambda^1 E_n^{(1)} + \lambda^2 E_n^{(2)} + \cdots \ , \tag{5}$$

where $|n^{(0)}\rangle$ is an eigenstate of the harmonic Hamiltonian in Eq. (1) and $E_n^{(0)}$ is the corresponding energy. In Paper I, we provided expressions for obtaining corrections to the zero-order energy for any order in the perturbation theory expansion k, $E_n^{(k)}$, and the corresponding corrections to the wave function, $|n^{(k)}\rangle$, using sparse linear algebra. In that work,

we also discussed the forms of $H^{(1)}$, $H^{(2)}$, and higher-order perturbations, and the reader is referred to Paper I for further discussion of the approach.

The effect of resonances on the results of VPT calculations is to cause the expansions in Eqs. (4) and (5) to either diverge or simply not to converge. Mechanistically, a resonance occurs between states $|n^{(0)}\rangle$ and $|m^{(0)}\rangle$ when a term term of the form $\langle n^{(0)}| H^{(k)} |m^{(0)}\rangle / (E_n^{(0)} - E_m^{(0)})$ becomes too large.

This term enters into the corrections to the wave functions for the first time at kth order as

$$\langle m^{(0)}|n^{(k)}\rangle = \frac{\langle n^{(0)}| H^{(k)} |m^{(0)}\rangle}{E_n^{(0)} - E_m^{(0)}} + \cdots \tag{6}$$

As the perturbation theory is taken to higher order, higher powers of the ratio in Eq. (6) will enter into the expressions for the corrections to the wave functions. When the ratio in Eq. (6) is large, the expansions in Eq. (4) and Eq. (5) may not converge. Therefore, it should be possible to use the size of the corrections to the wave functions to identify pairs of states that need to be treated by the deperturb and diagonalize approach.

More concretely, we know that at kth order the correction to the wave function for state n can be expressed as

$$|n^{(k)}\rangle = \sum_m \langle m^{(0)}|n^{(k)}\rangle |m^{(0)}\rangle \tag{7}$$

where the expansion coefficients, $\langle m^{(0)}|n^{(k)}\rangle$, are obtained through the approach detailed in Paper I. The terms that will become problematic are those for which $\langle m^{(0)}|n^{(k)}\rangle$ become large. Based on this, the states $|n^{(0)}\rangle$ and $|m^{(0)}\rangle$ are determined to be in resonance if

$$\chi^{\max} < \left|\langle m^{(0)}|n^{(k)}\rangle\right| \text{ or } \left|\langle n^{(0)}|m^{(k)}\rangle\right|. \tag{8}$$

This analysis leads to a series of pair-wise resonances, of the form $|n^{(0)}\rangle$ resonant with $|m^{(0)}\rangle$ and $|i^{(0)}\rangle$ resonant with $|j^{(0)}\rangle$. From these pairs of resonances, a graph of resonances can be built. This graph then provides the resonant spaces used in subsequent GVPT calculations. We call this method for the identification of resonances the wave function correction (WFC) approach.

In some cases, the WFC approach identifies resonances that are problematic. One such example occurs when there are low-frequency vibrations, and one obtains a non-terminating set of resonances between the state with one quantum of excitation in a high-frequency vibration and a series of states with one quantum in the same high-frequency vibration and

an increasing number of quanta in a low-frequency vibration. This has been described in a recent study by Stanton and co-workers.[25] Another problematic situation occurs for anharmonic oscillators, where the contributions from states with two or more quanta of excitation in a particular vibration contribute significantly to the description of the wave function for the state with one quantum of excitation in the same vibration. Most commonly, this occurs when a state with one quantum of excitation in a vibration that is well-described by a Morse oscillator is determined to be in resonance with the state with one additional quantum of excitation in that vibration. As noted above and illustrated in Tab. S2, a variational calculation based on a truncated quartic expansion of the Morse potential provides less accurate results than perturbation theory taken to second or higher order. Based on these observations, these sets of states should not be handled via deperturbation and diagonalization and should therefore not be considered to be in resonance. Given that these are frequently high-frequency motions, we follow the approach described in other works that use the Martin test and introduce an energy window to restrict which states are allowed to be in resonance.[25,43]

More specifically, for all of the results in this work we have introduced an energy window of $E^{\text{window}} = 500$ cm^{-1}. Only sets of states that span an energy range that is no larger than E^{window} will be considered to be in resonance. This is achieved by first identifying the value of χ^{max} for which the range of energies spanned by the identified resonance space is smaller than E^{window}. The value of χ^{max} is then reduced to the desired value, and states are reintroduced one by one so long as the range of energies spanned by the resonance space remains smaller than E^{window}. Every time a state is reintroduced the graph of resonances is reconstructed. If the originally identified resonance space has been divided into two or more sub-spaces, the energies spanned by pairs of subspaces are compared to E^{window}. In situations where the range is smaller then E^{window}, the subspaces are combined to make a larger space of nearly degenerate states.

The WFC approach resolves many of the challenges with identifying resonance spaces, discussed above. For one, it is general and can account for contributions to the expansion of the Hamiltonian from $H^{(2)}$, and higher-order perturbations as well as those from $H^{(1)}$. This allows us to treat both Darling-Dennison and Fermi resonances in an equivalent manner. Secondly, this approach will be sensitive to resonances that affect the intensities as well as the energies. Finally, χ^{max} is a dimensionless quantity and therefore treats high- and low-frequency modes equivalently. This is in contrast to the Martin threshold, χ^{Martin}, which has

units of energy. As vibrational frequencies commonly range over several orders of magnitude, a value for χ^{Martin} that works well in the higher frequency range may be too large when lower frequency vibrations are considered.

It is worth noting that similar conditions may be derived starting from canonical Van Vleck perturbation theory, but considering contributions to the Van Vleck transformation operators instead of the corrections to the wave functions.[41]

Moreover, the WFC threshold has an easy-to-understand meaning. A threshold value of 1.0 will only identify resonances involving states where the contributions as corrections to the wave function of interest are as larger or larger than the size of the zeroth order contribution. As perturbation theory assumes the corrections to the wave functions are small, a situation where the correction to the wave function is larger than the zero-order contribution is a clear indication of a breakdown in the method. By contrast, a threshold value of 0.5 will find corrections that have coefficients that are at least half the size of the coefficient of the zero-order state. Such large corrections are expected to affect the calculated spectrum, but are unlikely to lead to a breakdown of the perturbation theory.

Finally, there is a subtlety in the application of the Martin test that is of note. As outlined in Section S1 of the Supplemental Materials, the Martin test, for a given value of χ^{Martin}, is expressed as

$$\frac{\langle n^{(0)}|\, H^{(1)}\, |m^{(0)}\rangle^4}{|E_n^* - E_m^*|^3} \geq \chi^{\text{Martin}} \tag{9}$$

where E_n^* and E_m^* are the deperturbed energies, that is, the energies obtained from VPT2 where the coupling between $|n^{(0)}\rangle$ and $|m^{(0)}\rangle$ has been removed. This is obtained by comparing the eigenvalues of the matrix

$$\begin{pmatrix} E_n^* & \langle n^*|\, H\, |m^*\rangle \\ \langle n^*|\, H\, |m^*\rangle & E_m^* \end{pmatrix} \tag{10}$$

to the energies obtained by applying first-order perturbation theory to the states used to construct this matrix represntation of the Hamiltonian. Commonly, however, the approximation $(E_n^* - E_m^*) \approx (E_n^{(0)} - E_m^{(0)})$ is made.[25,42] This is justified in the case that states $|n^{(0)}\rangle$ and $|m^{(0)}\rangle$ have similar anharmonicities. As will be discussed below for *cc*-HOONO, this approximation does not always hold and can affect which resonances are identified in significant ways.

There is another type of significant resonance which will not be identified by the WFC

approach as presented here. In the construction of the matrix coupling the deperturbed states, it is possible for two states with significantly different harmonic frequencies to have similar deperturbed energies. When this is the case, even a small coupling matrix element can lead to a large amount of state mixing. Such situations can be identified by analysis of the anharmonic frequencies and re-running the VPT calculation that incorporates any possible resonances that have been identified by this analysis.

III. RESULTS AND DISCUSSION

Having detailed the WFC approach for identifying resonances, we turn now to assessing its performance. We start by an application of the method to a series of molecules, which were chosen because they illustrate several common ways in which the treatment of resonances can affect the calculated vibrational spectra. Next, we will investigate how the performance of the WFC method depends on the value of its adjustable parameter, $\chi^{\max}$. Finally, we will compare resonances identified by the WFC approach to those found when the Martin test is used.

A. Applications of the WFC Method

In Fig. 1, the results of performing second-order vibrational perturbation theory (VPT2) calculations of the spectra of CH_4, H_2CO, HNO_3, and cc-HOONO are provided, with the corresponding structures shown in the insets. In panels (a), (c), (e), and (g) the calculated spectra obtained from standard, non-degenerate perturbation theory calculations (SVPT, red) are compared to those obtained from GVPT calculations (blue), while in in panels (b), (d), (f), and (h) the spectra from SVPT calculations are compared to those obtained from deperturbed VPT calculations (DVPT, green). The frequencies and intensities used to generate these spectra are provided in Tabs. S3-S6. All of these systems have been studied previously, including with VPT,[35,37,55–59] and were chosen for this study as they broadly demonstrate the types of resonance effects common in vibrational problems. All results were evaluated using a partial quartic force field obtained using the Gaussian 16 software package at the MP2/aug-cc-pVTZ level of theory and basis.[44,60] All VPT2 calculations were performed using the PyVibPTn implementation of internal coordinate vibrational pertur-

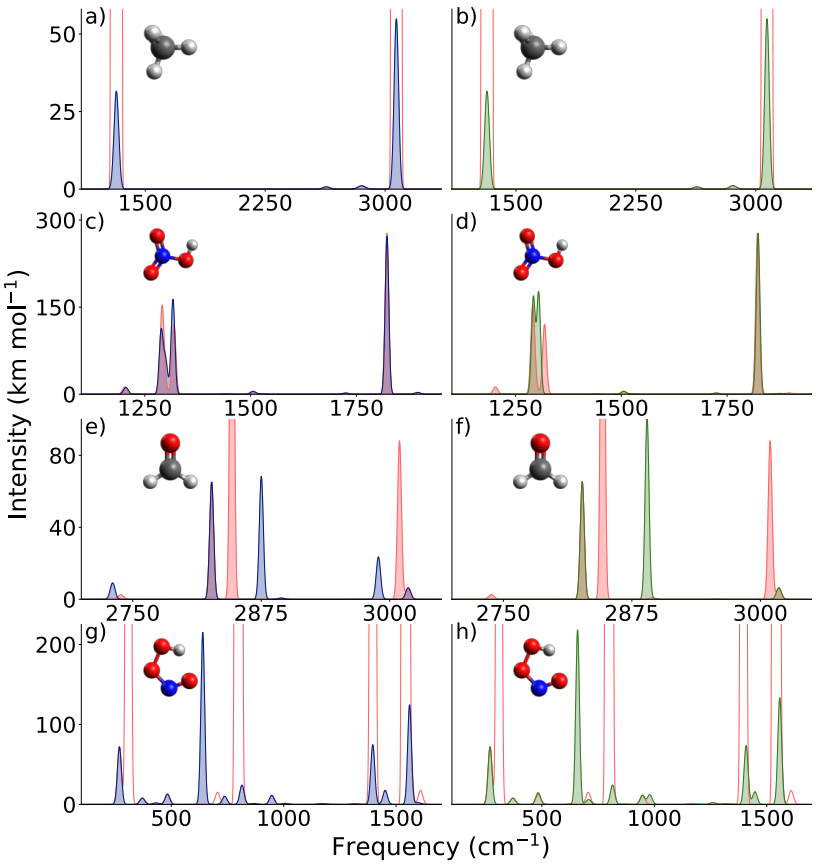

FIG. 1. Vibrational spectra from GVPT (blue, left), DVPT (green, right), and SVPT (red) calculations for CH_4 (a and b), HNO_3 (c and d), H_2CO (e and f), and cc-HOONO (g and h). Resonances are identified by the WFC approach with $\chi^{\max} = 0.3$ and the corresponding transitions and intensities are provided in Tabs. S3–S6.

bation theory described in Paper I based on normal modes comprised of linear combinations of internal coordinates.[53,61] The corresponding z-matrices and equilibrium geometries are provided in Tab. S2.

In CH_4 (panels (a) and (b) in Fig. 1), three of the CH stretches are degenerate, but they are decoupled as they have different symmetries. However, the use of polyspherical (z-matrix) coordinates to define the normal modes leads to an inequivalence in the treatment of the six HCH angles. This results in the calculation being performed under C_{2v} symmetry rather than the full T_d symmetry of the molecule. As a result, small errors from the numerical evaluation of the coefficients of the cubic and quartic terms in the potential can lead to a loss of the expected symmetry. This type of numerical artifact and the corresponding effects are

discussed in a recent work.[60] This numerical symmetry breaking is evident in the coupling matrix used in the GVPT calculations that is obtained by applying DVPT to the three states with one quantum of excitation in any of the degenerate CH stretching vibrations. By symmetry, the coupling matrix element between any pair of these states should be zero. In practice, these matrix elements are ~ 0.001 cm^{-1}, which while very small and consistent with errors from numerical differentiation they are large enough to break the symmetry of degenerate vibrations. This in turn will significantly affect the corrections to the wave functions. The degenerate states are coupled through $H^{(2)}$. This will affect the second order correction to the wave function, but not the second order correction to the energy. This is reflected in the nearly identical values of the energies obtained from SVPT and GVPT calculations. On the other hand, the second order correction to the wave function will contribute to the calculated intensities of transitions to states with one quantum of excitation. When these degeneracies are not accounted for, some of the intensities are calculated to be larger than 60 000 km mol^{-1} (red). It is possible to avoid this type of issue by only allowing states with the same symmetry to couple. However it is desirable to have a method that handles these types of numerical artifacts automatically.

When we compare the spectra evaluated from GVPT and SVPT calculations of HNO_3, shown in Fig. 1(c) and (d), we find only small differences in the calculated transition frequencies. In contrast to CH_4, due to the lack of exact degeneracies, when resonances are introduced the spectra of HNO_3 also display only small changes in the transition intensities. The primary differences between the two spectra shown in panel (c) of Fig. 1 occur near 1300 cm^{-1}, where there is a decrease in intensity in the peak at 1290 cm^{-1} and an increase in the intensity of the peak at 1315 cm^{-1} in the spectrum obtained from the GVPT calculation (blue) compared to that obtained from the SVPT calculation (red). These changes in intensity reflect the effects of two distinct resonances on the spectra obtained from VPT2 calculations.

The small decrease in the intensity of the peak at 1290 cm^{-1} results from a coupling between the state with one quantum of excitation in mode 4 and the state with two quanta of excitation in mode 7. These states have energies of 1292 and 1295 cm^{-1}, respectively, based on the DVPT2 calculation (See Fig. S2 for illustrations of these normal modes). The coupling of this pair of states provides an example of a Fermi resonance. Here the transition to the state with one quantum of excitation in mode 4 has a large intensity based on the

harmonic and DVPT calculations, while the transition to the state with two quanta in mode 7 has little intensity. On the other hand, the energy difference between these two states is only 15 cm^{-1} based on the harmonic calculations. This leads the SVPT calculation to provide a poor description of the intensities of these two transitions, as well as the shoulder that develops on this peak when GVPT is used to calculate the spectrum that is not seen in the results of the SVPT calculation.

The second intensity difference between the three VPT calculations is seen near 1315 cm^{-1}. These changes reflect a decrease in the intensity of the transition to the state with one quantum of excitation in mode 3, when this state is allowed to couple to the state with one quantum of excitation in both modes 6 and 9 in a GVPT calculation. Interestingly, both the GVPT and SVPT calculations give an intensity of the transition to the state with one quantum of excitation in modes 6 and 9 of $\sim$12 km mol^{-1}. At the same time the intensity of the transition to the state with one quantum of excitation in mode 3 increases from a value of 120 km mol^{-1} based on a SVPT calculation to 163 km mol^{-1} from a GVPT calculation. Moreover when a DVPT calculation is used to evaluate the spectrum, the intensities of the transitions to these two states become 0.5 km mol^{-1} and 174 km mol^{-1}, respectively. The fact that when SVPT to GVPT are used to calculate the spectrum, the intensity of transition to the state with one quantum of excitation in mode 3 increases so significantly while the intensity of the transition to the state with one quantum of excitation in modes 6 and 9 remains the same is a manifestation of the fact that the leading contribution to the corrections to the intensity for transitions to these two states arises from different orders in the correction to the wave function. In particular, the leading contribution to the $\sim$50 km mol^{-1} change in the intensity of the transition to the state with one quantum in mode 3 when it is calculated using DVPT and SVPT comes from the treatment of the second order correction to the wave function, which includes contributions that are quadratic in the ratio of matrix elements of $H^{(1)}$ and the difference between the harmonic energies. This correction will be more sensitive to possible near degeneracies than the first order correction to the wave function, which provides the leading contribution to the difference in the intensity of the transition to the state with one quantum of excitation in modes 6 and 9 when it is calculated using SVPT and DVPT.

As has been noted in prior studies,[35,55] there are important resonances that must be handled in H_2CO. These resonances lead to a modulation of both the frequencies and

intensities in the spectrum of H_2CO (panels (e) and (f) of Fig. 1).There is a well-known triad of near-degeneracies between the state with one quantum of excitation in mode 5, the state with one quantum of excitation both modes 2 and 6, and the state with one quantum of excitation both modes 3 and 6 (see Fig. S3 for illustrations of these vibrations). In the absence of resonance handling, these near degeneracies lead to a large shift in the frequency of mode 5, going from 3009 cm^{-1} when applying SVPT to 2875 cm^{-1} when using GVPT. The near degeneracies also lead to a more than an order of magnitude change in the intensity of the transition to the state with one quantum in both modes 2 and 6, decreasing from 344 km mol^{-1} (SVPT) to 24 km mol^{-1} (GVPT).

For cc-HOONO (panels (g) and (h) in Fig. 1), the effects of resonances are most dramatic and there are also significant differences between the spectra obtained with and without resonance handling. In the spectrum obtained from a SVPT calculation, there are multiple peaks with intensities exceeding 5000 km mol^{-1}. In the spectrum obtained from the GVPT calculation, the largest transition intensity in this spectral region is around 120 km mol^{-1}. There are also a large number of smaller peaks that are found in the spectrum that was obtained with GVPT that do not appear in the spectrum obtained from the SVPT calculation.

For the four systems discussed here, there are many benefits to the use of an automated approach that accounts for the effects of resonances on the wave functions as well as the energies, like the WFC method. In the case of the CH stretches in CH_4, it provides a safeguard against unexpected symmetry breaking, which results from small numerical artifacts. For HNO_3, it identifies resonances with subtle but important effects on the spectrum. For H_2CO and cc-HOONO, the WFC approach identifies the resonance interactions that lead to the divergence of the intensities when SVPT is used to calculate the spectrum.

B. Analysis of Performance of the WFC Method

The question naturally arises as to how the resonances identified by the WFC approach depend on the value of $\chi^{\max}$. For the calculations discussed above $\chi^{\max} = 0.3$, which we have found to be a good choice in most situations. To interrogate the effect of changing the value of $\chi^{\max}$, we will use H_2CO as a test system, as there are multiple important resonances that affection the VPT2 calculation of its vibrational spectrum. When labeling states, we will

borrow notation from Romanowski *et al.*[55] and use $|i_n\rangle^{(0)}$ to indicate the zero-order state with n quanta of excitation in mode i and $|i_n j_m\rangle^{(0)}$ to indicate the state with n quanta in mode i and m in mode j. In H_2CO, mode 1 is the symmetric CH stretch, mode 2 is the CO stretch, mode 3 is the HCH bend, mode 4 is the out-of-plane motion of the hydrogen atoms, mode 5 is the anti-symmetric CH stretch, and mode 6 is the in-plane rocking motion of the CH bonds. These motions are illustrated in Fig. S3. Comparing the harmonic frequencies of these vibrations, one finds that the frequencies of the CH stretching vibrations, modes 1 and 5, are each roughly twice the frequencies of each of the other four vibrations. This leads to an approximate good quantum number based on the number of quanta of excitation in each individual vibration

$$N_t = 2(n_1 + n_5) + n_2 + n_3 + n_4 + n_6, \tag{11}$$

which is proportional to the energy.

In Fig. 2, the calculated vibrational spectra for H_2CO, which are obtained from GVPT calculations with $\chi^{\max}$ (blue) ranging from 0.1 to 1.0 are compared to the vibrational spectra obtained when considering the resonances derived from the polyad quantum number that is defined in Eq. (11) (red). This polyad represents the most complete set of resonances that make sense to incorporate in a GVPT calculation for H_2CO.

When $\chi^{\max} = 1.0$, corresponding to a wave function correction equal to the contribution from the zero-order state itself, we identify only one resonance: the one that involves the state with one quantum of excitation in the anti-symmetric CH stretch $|5_1\rangle^{(0)}$, and the state with one quantum of excitation in both the CH in-plane rocking motion and the CO stretch, $|6_1 2_1\rangle^{(0)}$. This resonance reflects the near-degeneracy of these states at the harmonic level. These two states have harmonic frequencies of 3047 and 3020 cm^{-1}, respectively, and the coupling matrix element between these states is 57 cm^{-1}, resulting in an overlap between $|6_1 2_1\rangle^{(0)}$ and $|5_1\rangle^{(1)}$ of 2.1.

When $\chi^{\max}$ is reduced to 0.5 no additional resonances are identified, while for $0.2 < \chi^{\max} < 0.4$ we identify a second resonance, which involves $|6_1 2_1\rangle^{(0)}$ and $|6_1 3_1\rangle^{(0)}$. This is illustrated in Fig. 2 and Tab. I. The additional resonance that is identified when $\chi^{\max} < 0.4$ comes from coupling between $|6_1 2_1\rangle^{(0)}$ and $|6_1 3_1\rangle^{(0)}$ through $H^{(2)}$. Importantly, despite its small coupling to the bright $|5_1\rangle^{(0)}$ state and despite the relatively small concomitant shift in the transition energy (8 cm^{-1}) the intensity of the transition to the $|6_1 3_1\rangle^{(0)}$ state nearly

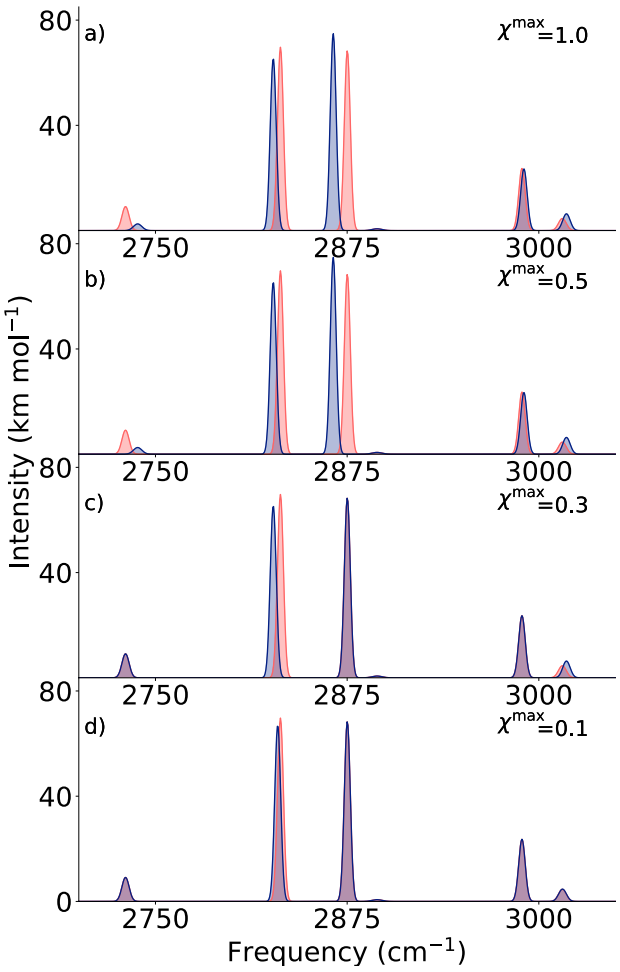

FIG. 2. Vibrational spectra for H_2CO with $\chi^{max} = 1.0$ (a), 0.5 (b), 0.3 (c), and 0.1 (d) (blue) compared to the spectrum obtained using the polyad defined by Eq. (11) (red). The corresponding resonant spaces for degeneracy handling are provided in Tab. I.

quadruples when this resonance is introduced.

Finally, at a χ^{max} value of 0.1 (panel (d) in Fig. 2) the algorithm identifies an additional set of resonances that includes the $|1_1\rangle^{(0)}$, $|3_2\rangle^{(0)}$, and $|3_1 2_1\rangle^{(0)}$ states. Such resonances are anticipated by the ubiquity of strong Fermi resonances between CH stretching vibrations and the associated HCH bends,[25,62] although in the case of H_2CO the resonance is admittedly weak. The origin of the resonance interaction between the stretch fundamental $|1_1\rangle^{(0)}$ and bend overtone $|3_2\rangle^{(0)}$ is the small but significant coupling matrix element of 25 cm^{-1} with a modest sized difference in the harmonic frequencies, being separated by around 90 cm^{-1}. Looking at the displacement vectors provided in Fig. S3, mode 2 also has contributions

TABLE I. Resonant spaces for H_2CO that are identified by the WFC approach for specified values of $\chi^{\max}$ as well as the transition frequencies and intensities obtained from the resulting GVPT calculation. Resonance spaces are grouped by symmetry. The corresponding spectra are plotted in Fig. 2.

	B_2[a]			A_1[a]		
$\chi^{\max}$	State	Frequency (cm^{-1})	Intensity (km mol^{-1})	State	Frequency (cm^{-1})	Intensity (km mol^{-1})
1.0	$\|5_1\rangle^{(0)}$	2866	74.87	$\|1_1\rangle^{(0)}$[b]	2827	65.48
	$\|6_1 2_1\rangle^{(0)}$	2990	23.50			
0.5	$\|5_1\rangle^{(0)}$	2866	74.87	$\|1_1\rangle^{(0)}$[b]	2827	65.48
	$\|6_1 2_1\rangle^{(0)}$	2990	23.50			
0.3	$\|5_1\rangle^{(0)}$	2875	68.36	$\|1_1\rangle^{(0)}$[b]	2827	65.48
	$\|6_1 3_1\rangle^{(0)}$	2730	9.14			
	$\|6_1 2_1\rangle^{(0)}$	2989	23.62			
0.1	$\|5_1\rangle^{(0)}$	2875	68.36	$\|1_1\rangle^{(0)}$	2829	67.02
	$\|6_1 3_1\rangle^{(0)}$	2730	9.14	$\|3_2\rangle^{(0)}$	3015	4.68
	$\|6_1 2_1\rangle^{(0)}$	2989	23.62	$\|3_1 2_1\rangle^{(0)}$	3221	0.49

[a] B_2 corresponds to the space of resonant states with B_2 symmetry while A_1 corresponds to the states with A_1 symmetry.

[b] No resonances with this state are identified at this threshold.

from the HCH bending vibration. Thus the couplings among these three states can be interpreted to be a classic stretch-bend Fermi resonance, where the HCH bend contribution is distributed over two normal modes.

As noted above, we have found that a value for $\chi^{\max}$ of around 0.3 is effective. At this value, we recover both the resonances that cause the perturbation theory to break down

as well as the weaker resonances that still have a notable effect on the spectrum. It is possible that going to a smaller value of $\chi^{\max}$ would lead to the inclusion of more relevant resonances, however the effect of these resonances will be small. As can be seen in Fig. 2(d), where the spectra obtained using $\chi^{\max} = 0.1$ and when N_t in Eq. (11) is used to define the set of resonances, it is difficult to detect any significant differences between the spectra calculated by these two approaches. Moreover, by increasing the size of the resonant space, we come closer to the limit of performing a variational calculation with a quartic force-field. Not only will such a variational calculation be more computationally intensive than a VPT calculation, it can be expected to yield poorer results than VPT since the Hamiltonian is expressed as a quartic expansion.

C. Comparison to the Martin Test

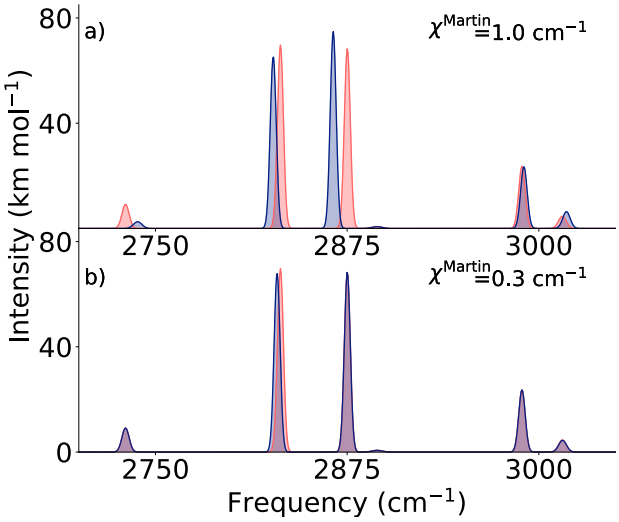

FIG. 3. Vibrational spectra for H_2CO with resonances identified by the Martin test with $\chi^{\text{Martin}} = 1.0$ cm^{-1} (a) and $\chi^{\text{Martin}} = 0.3$ cm^{-1} (b) (blue) compared to the spectrum obtained using the polyad defined by Eq. (11) (red). The corresponding resonant spaces for degeneracy handling are provided in Tab. S7 and spectra obtained when other values of χ^{Martin} are used can be found in Fig. S5.

It is also important to note how the WFC method compares to commonly used approaches, specifically the Martin test. The Martin test and its derivation are outlined in

the Supplemental Materials. In comparing the WFC approach and the Martin test, we will again consider H_2CO. The results of applying the Martin test with values of χ^{Martin} ranging from 0.1 cm^{-1} to 1.0 cm^{-1} are plotted in Fig. 3 and Fig. S5 and the corresponding frequencies and intensities are provided in Tab. S7.

A commonly used value for the threshold energy for the Martin test, χ^{Martin}, is 1.0 cm^{-1}. When this value is used the only resonance in H_2CO identified is between $|5_1\rangle^{(0)}$ and $|6_1 2_1\rangle^{(0)}$. This is the same resonance that is identified when $\chi^{\text{max}} > 0.4$. When χ^{Martin} is lowered to 0.3 cm^{-1}, the $|6_1 3_1\rangle^{(0)}$ state is added to the resonace space. This generates the same resonance space that was identified by the WFC approach when $\chi^{\text{max}} < 0.4$. For $\chi^{\text{Martin}} = 1.0$ cm^{-1}, no resonances are identified that involve symmetric CH stretch. This is similar to the results of the WFC approach with $\chi^{\text{max}} > 0.2$. Once χ^{Martin} is decreased a value of 0.3 cm^{-1}, the resonance between the $|1_1\rangle^{(0)}$ and $|3_2\rangle^{(0)}$ states is identified, the $|3_1 2_1\rangle^{(0)}$ state, remains unidentified even when $\chi^{\text{Martin}} = 0.1$ cm^{-1}.

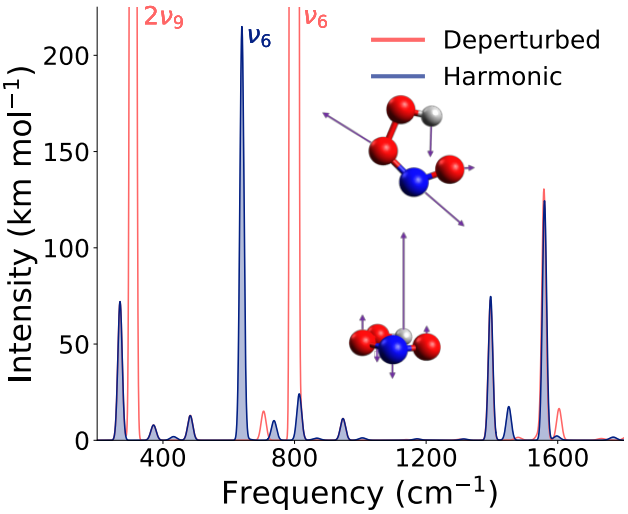

FIG. 4. Simulated spectrum for cc-HOONO using the Martin test with a threshold value of 1 cm^{-1} with the denominator in Eq. (9) determined by either the harmonic frequency difference (blue) or the deperturbed energy difference (red). When using the deperturbed energy difference the resonance between the ON stretch (mode 6, top inset) and the overtone in the out-of-phase combination of the out-of-plane hydrogen and nitrogen motions (mode 9, bottom inset) is not identified. This leads to the state with one quantum of excitation in mode 6 and the state with two quanta of excitation in mode 9 having unphysically large intensities.

In cc-HOONO, there is a near-degeneracy between the state with two quanta of excitation in mode 9 and the state with one quantum of excitation in mode 6. The displacement vectors for these motions are illustrated in the insets in Fig. 4. If this resonance is not included in the VPT treatment, the intensity of the transition to the state with one quantum of excitation in mode 6 exceeds 5000 km mol^{-1}. Interestingly, the ability of the Martin test to identify this resonance depends on the form of the denominator in Eq. (9). As noted in the discussion of the Martin test in the Supplemental Materials, the working equations rely on the assumption that the energy difference between the two coupled states is the same when these energies are evaluated at the harmonic level or based on the deperturbed energies. The choice of which energy difference to use is unclear and often the difference between the deperturbed energies is used. As seen in Fig. 4, if the difference between the harmonic frequencies is used the resonance is identified when $\chi^{\text{Martin}} = 1.0$ cm^{-1}. The same threshold will not capture this resonance if the deperturbed energies are used, as is seen by the large intensities of two of the transitions in the specrum shown in red. This reflects the large differences between the anharmonicities of the out-of-plane motions (mode 9) and the ON stretch (mode 6). This subtlety is obviated in the WFC approach as there is no ambiguity since the energy difference is accounted for directly in the corrections to the wave functions.

IV. CONCLUSION

The choice of resonance interactions considered in vibrational perturbation theory calculations can have a significant effect on the simulated spectrum. By focusing on the corrections to the wave functions, as provided by the approach described in Paper I, it is possible to develop a method for the identifying resonances that is straightforward and effective and which does not have the ambiguity of the Martin test with respect to the energies used to evaluate the denominator in Eq. (9). This approach, which we call the wave function correction approach (WFC), identifies the same important resonances as existing methodologies, while allowing for the identification of both Fermi and Darling-Dennison resonances with a single test. It has been shown to be effective in identifying important resonances in both H_2CO and cc-HOONO, and the algorithm as presented generalizes cleanly to arbitrary order in perturbation theory. It has also been shown by Stanton and coworkers that a mixed approach to the identification of resonances where polyads are combined with

automatic identification can provide a powerful method for the identification of all important resonances.[25] The WFC approach, and its implementation in the PyVibPTn[61] package for vibrational perturbation theory is well-suited to this type of extension, and can inform approaches using polyad quantum numbers and other approaches.

AUTHOR DECLARATIONS

Conflict of Interest

The authors have no conflicts to disclose.

DATA AVAILABILITY

The data that supports the findings of this study are available within the article and its supplementary material.

AUTHOR CONTRIBUTIONS

Anne B. McCoy: Conceptualization (lead); Funding acquisition (lead); Resources (lead); Supervision (lead); Methodology (equal); Writing – original draft (equal). **Mark A. Boyer**: Software (lead); Formal analysis (lead); Investigation (lead); Visualization (lead); Methodology (equal); Writing – original draft (equal).

ACKNOWLEDGMENT

The authors acknowledge support from the Chemistry Division of the National Science Foundation (CHE-1856125 for scientific work and CHE-2154126 for code development). Parts of this work were performed using the Ilahie cluster at the University of Washington, which was purchased using funds from a MRI grant from the National Science Foundation (CHE-1624430). This work was also facilitated through the use of advanced computational, storage, and networking infrastructure provided by the Hyak supercomputer system and funded by the STF at the University of Washington.

SUPPLEMENTARY MATERIAL

See the supplementary material for a description of the Martin test; table containing the $z-$matrix and equlibrium geometries of the molecules considered in this study; tables of frequencies and intensities for the spectra provided in this study; visualizations of relevant normal modes for CH_4, H_2CO, HNO_3, and cc-HOONO; spectra and tables of frequencies and intensities for H_2CO with resonances identified using different threshold values for the Martin test.

REFERENCES

[1]E. B. Wilson, J. C. Decius, and P. C. Cross, *Molecular Vibrations* (Dover, New York, 1955).

[2]V. Barone, S. Alessandrini, M. Biczysko, J. R. Cheeseman, D. C. Clary, A. B. McCoy, R. J. DiRisio, F. Neese, M. Melosso, and C. Puzzarini, Nature Reviews Methods Primers **1**, 38 (2021).

[3]J. M. Bowman, ed., *Vibrational Dynamics of Molecules* (World Scientific, New Jersey, 2022).

[4]D. T. Colbert and W. H. Miller, J. Chem. Phys. **96**, 1982–1991 (1992).

[5]J. C. Light and T. Carrington, "Discrete-variable representations and their utilization," in *Advances in Chemical Physics*, edited by S. A. Rice (Wiley-Blackwell, 2007) pp. 263–310.

[6]B. R. Henry, Acc. Chem. Res. **10**, 207–213 (1977).

[7]E. L. Sibert, J. T. Hynes, and W. P. Reinhardt, J. Chem. Phys. **77**, 3595 (1982).

[8]M. S. Child and R. T. Lawton, Faraday Discuss. Chem. Soc. **71**, 273–285 (1981).

[9]R. Dawes and T. Carrington, J. Chem. Phys. **121**, 726–736 (2004).

[10]D. Luckhaus, J. Chem. Phys. **113**, 1329–1347 (2000).

[11]X. G. Wang and T. Carrington, J. Chem. Phys. **130** (2009), 10.1063/1.3077130.

[12]J. M. Bowman, Acc. Chem. Res. **19**, 202–208 (1986).

[13]J. M. Bowman, S. Carter, and X. Huang, Int. Rev. Phys. Chem. **22**, 533–549 (2003).

[14]J. M. Bowman, T. Carrington, and H. D. Meyer, Mol. Phys. **106**, 2145–2182 (2008).

[15]H.-D. Meyer, U. Manthe, and L. S. Cederbaum, Chem. Phys. Lett. **165**, 73–78 (1990).

[16]H. Meyer, WIREs Comput Mol Sci **2**, 351–374 (2012).

[17]A. P. Scott and L. Radom, J. Chem. Phys. **100**, 16502–16513 (1996).

[18]A. Adel and D. M. Dennison, Phys. Rev. **43**, 716–723 (1933).

[19]W. H. Shaffer, H. H. Nielsen, and L. H. Thomas, Phys. Rev. **56**, 895 (1939).

[20]H. H. Nielsen, Phys. Rev. **60**, 794–810 (1941).

[21]R. C. Herman and W. H. Shaffer, J. Chem. Phys. **16**, 453 (1948).

[22]H. H. Nielsen, Rev. Mod. Phys. **23**, 90–136 (1951).

[23]E. L. Sibert, J. Chem. Phys. **88**, 4378–4390 (1988).

[24]V. Barone, J. Chem. Phys. **122**, 014108 (2005).

[25]P. R. Franke, J. F. Stanton, and G. E. Douberly, J. Phys. Chem. A **125**, 1301–1324 (2021).

[26]P. M. Morse, Phys. Rev. **34**, 57–64 (1929).

[27]M. L. Grenier-Besson, G. Amat, and H. H. Nielsen, J. Chem. Phys. **36**, 3454 (1962).

[28]H. H. Nielsen, Phys. Rev. **68**, 181 (1945).

[29]R. D. Amos, N. C. Handy, W. H. Green, D. Jayatilaka, A. Willetts, and P. Palmieri, J. Chem. Phys. **95**, 8323 (1998).

[30]L. C. Dzugan, J. Matthews, A. Sinha, and A. B. McCoy, J. Phys. Chem. A **121**, 9262–9274 (2017).

[31]J. Bloino and V. Barone, J. Chem. Phys. **136**, 124108 (2012).

[32]J. Z. Gong, D. A. Matthews, P. B. Changala, and J. F. Stanton, J. Chem. Phys. **149**, 114102 (2018).

[33]J. Sakurai, *Modern Quantum Mechanics - Revised Edition* (Addison-Wesley Pub. Co, Reading, Massachusetts, 1994).

[34]D. M. Dennison, Phys. Rev. **41**, 304 (1932).

[35]E. L. Sibert, J. Chem. Phys. **90**, 2672–2683 (1989).

[36]M. E. Kellman, J. Chem. Phys. **93**, 6630 (1990).

[37]S. V. Krasnoshchekov and N. F. Stepanov, J. Chem. Phys. **139**, 184101 (2013).

[38]J. F. Gaw, A. Willetts, W. H. Green, and N. C. Handy, "Spectro version 3.0," in *Advances in Molecular Vibrations and Collision Dynamics*, Vol. 1B, edited by J. M. Bowman (JAI Press, Greenwich, CT, 1990).

[39]J. F. Stanton, J. Gauss, L. Cheng, M. E. Harding, D. A. Matthews, and P. G. Szalay, "CFOUR, coupled-cluster techniques for computational chemistry, a quantum-chemical program package," (2010), With contributions from A.A. Auer, A. Asthana, R.J. Bartlett, U. Benedikt, C. Berger, D.E. Bernholdt, S. Blaschke, Y. J. Bomble, S. Burger, O. Chris-

tiansen, D. Datta, F. Engel, R. Faber, J. Greiner, M. Heckert, O. Heun, M. Hilgenberg, C. Huber, T.-C. Jagau, D. Jonsson, J. Jusélius, T. Kirsch, K. Klein, G.M. KopperW.J. Lauderdale, F. Lipparini, J. Liu, T. Metzroth, L.A. Mück, D.P. O'Neill, T. Nottoli, D.R. Price, E. Prochnow, C. Puzzarini, K. Ruud, F. Schiffmann, W. Schwalbach, C. Simmons, S. Stopkowicz, A. Tajti, J. Vázquez, F. Wang, J.D. Watts and the integral packages MOLECULE (J. Almlöf and P.R. Taylor), PROPS (P.R. Taylor), ABACUS (T. Helgaker, H.J. Aa. Jensen, P. Jørgensen, and J. Olsen), and ECP routines by A. V. Mitin and C. van Wüllen. For the current version, see http://www.cfour.de.

[40]D. A. Matthews and J. F. Stanton, Mol. Phys. **107**, 213–222 (2009).

[41]S. V. Krasnoshchekov, E. V. Isayeva, and N. F. Stepanov, J. Chem. Phys. **141**, 234114 (2014).

[42]J. M. L. Martin, T. J. Lee, P. R. Taylor, and J. P. François, J. Chem. Phys. **103**, 2589–2602 (1995).

[43]Q. Yang, M. Mendolicchio, V. Barone, and J. Bloino, Front. Astron. Space Sci. **8**, 665232 (2021).

[44]M. J. Frisch, G. W. Trucks, H. B. Schlegel, G. E. Scuseria, M. A. Robb, J. R. Cheeseman, G. Scalmani, V. Barone, G. A. Petersson, H. Nakatsuji, X. Li, M. Caricato, A. V. Marenich, J. Bloino, B. G. Janesko, R. Gomperts, B. Mennucci, H. P. Hratchian, J. V. Ortiz, A. F. Izmaylov, J. L. Sonnenberg, D. Williams-Young, F. Ding, F. Lipparini, F. Egidi, J. Goings, B. Peng, A. Petrone, T. Henderson, D. Ranasinghe, V. G. Zakrzewski, J. Gao, N. Rega, G. Zheng, W. Liang, M. Hada, M. Ehara, K. Toyota, R. Fukuda, J. Hasegawa, M. Ishida, T. Nakajima, Y. Honda, O. Kitao, H. Nakai, T. Vreven, K. Throssell, J. A. Montgomery, Jr., J. E. Peralta, F. Ogliaro, M. J. Bearpark, J. J. Heyd, E. N. Brothers, K. N. Kudin, V. N. Staroverov, T. A. Keith, R. Kobayashi, J. Normand, K. Raghavachari, A. P. Rendell, J. C. Burant, S. S. Iyengar, J. Tomasi, M. Cossi, J. M. Millam, M. Klene, C. Adamo, R. Cammi, J. W. Ochterski, R. L. Martin, K. Morokuma, O. Farkas, J. B. Foresman, and D. J. Fox, "Gaussian 16 revision c.01," (2016), Gaussian Inc. Wallingford CT.

[45]B. T. Darling and D. M. Dennison, Phys. Rev. **57**, 128 (1940).

[46]J. Vázquez and J. F. Stanton, Mol. Phys. **105**, 101–109 (2007).

[47]M. Toyama, T. Oka, and Y. Morino, Journal of Molecular Spectroscopy **13**, 193–213 (1964).

[48]A. Willetts, N. C. Handy, W. H. Green, and D. Jayatilaka, J. Phys. Chem. **94**, 5608–5616 (1990).

[49]J. Vázquez and J. F. Stanton, Mol. Phys. **104**, 377–388 (2006).

[50]M. A. Boyer and A. B. McCoy, J. Chem. Phys. **156**, 054107 (2022).

[51]T. Kato, *Perturbation Theory for Linear Operators* (Springer-Verlag, New York, 1976).

[52]A. S. Hansen, T. Bhagde, Y. Qian, A. Cavazos, R. M. Huchmala, M. A. Boyer, C. F. Gavin-Hanner, S. J. Klippenstein, A. B. McCoy, and M. I. Lester, J. Chem. Phys. **156**, 014301 (2022).

[53]S. J. Stropoli, T. Khuu, M. A. Boyer, N. V. Karimova, C. Gavin-Hanner, S. Mitra, A. L. Lachowicz, N. Yang, R. B. Gerber, A. B. McCoy, and M. A. Johnson, J. Chem. Phys. **156**, 174303 (2022).

[54]S. J. Stropoli, T. Khuu, J. P. Messinger, N. V. Karimova, M. A. Boyer, I. Zakai, S. Mitra, A. L. Lachowicz, N. Yang, S. C. Edington, R. B. Gerber, A. B. McCoy, and M. A. Johnson, J. Phys. Chem. Lett. **13**, 2750–2756 (2022).

[55]H. Romanowski, J. M. Bowman, and L. B. Harding, J. Chem. Phys. **82**, 4155 (1985).

[56]Y. Miller, G. M. Chaban, and R. B. Gerber, Chem. Phys. **313**, 213–224 (2005).

[57]E. X. Li, I. M. Konan, M. I. Lester, and A. B. McCoy, J. Phys. Chem. A **110**, 5607–13 (2006).

[58]X. Zhang, M. R. Nimlos, G. B. Ellison, M. E. Varner, and J. F. Stanton, J. Chem. Phys. **124**, 084305 (2006).

[59]X. Zhang, M. R. Nimlos, G. B. Ellison, M. E. Varner, and J. F. Stanton, J. Chem. Phys. **126**, 174308 (2007).

[60]A. B. McCoy and M. A. Boyer, "Exploring expansions of the potential and dipole surfaces used for vibrational perturbation theory," submitted to *J. Phys. Chem. A*, Aug. 11, 2022.

[61]M. A. Boyer and A. B. McCoy, "PyVibPTn, a general package for vibrational perturbation theory," (2021), accessed 2022/6/4, 10.5281/zenodo.5563091.

[62]E. G. Buchanan, J. C. Dean, T. S. Zwier, and E. L. Sibert, J. Chem. Phys. **138**, 064308 (2013).